Identification of Hammerstein Systems Using Preisach Model for Sticky Control Valves

Lei Fang and Jiandong Wang*

College of Engineering, Peking University, Beijing 100871, China

ABSTRACT: This Article is motivated by identification of sticky control valves under oscillatory or general types of input signals in feedback control loops. A novel Hammerstein system with Preisach model as the input nonlinearity is proposed to capture the behavior of sticky control valves followed by linear dynamic subsystems. Preisach model is flexible for capturing complicated signatures of sticky control valves, and encloses the data-driven stiction models, which describe the behaviors of sticky control valves in oscillations, as special cases. A regularized iterative method is proposed to identify the Hammerstein systems. The persistently exciting (PE) condition for identification of Preisach model is established for oscillatory input signals, after showing that a known sufficient PE condition established for general input signals is not satisfied by oscillatory signals. Simulated, experimental, and industrial examples are provided to support the obtained results.

1. INTRODUCTION

Control valves in process industries possibly present various nonlinearities, which may degrade control performance or even cause oscillations arisen in closed-control loops. Industrial surveys[1−3] indicate that about 20−30% of control loops oscillate due to valve nonlinearities, such as stiction, hysteresis, deadband, or deadzone. Among those nonlinearities, valve stiction, resulting from the significant difference between kinetic and static frictions, is most commonly encountered. Hence, the detection, quantification, and compensation of control valve stiction have been very active research topics recently.[4] If the input $u(t)$ and output $x(t)$ of the control valve are measurable, then the control valve stiction is clearly revealed by plotting $x(t)$ against $u(t)$ to formulate a signature plot. However, many control valves in industrial practice do not provide the measurement of $x(t)$ (the valve position), so that the signature of control valves is not easy to obtain. In this case ($x(t)$ is unmeasurable), the methods based on Hammerstein system identification perhaps have the best performance in detecting control valve stiction[4] (Chapter 13 therein).

Hammerstein system is composed of a static input nonlinearity followed by a linear time-invariant (LTI) subsystem, and has been widely used as a mathematical model to describe many physical systems.[5,6] However, to model sticky control valves, the static input nonlinearity needs to be extended into the one with memory effects. Srinivasan et al.[7] applied the idea of separable least-squares to a stiction model parametrized by one parameter. Jelali,[8] Choudhury et al.,[9] Karra and Karim,[10] Ivan and Lakshminarayanan,[11] Qi and Huang,[12] Romanno and Garcia,[13] Farenzena and Trierweiler,[14] and Capaci and Scali[15] identified the Hammerstein systems by using various data-driven stiction models with two parameters. Nallasivam et al.[16] identified the stiction model parametrized by one parameter followed by a nonlinear dynamic subsystem instead of a linear one. In all of these cited articles, the control valve stiction is represented by data-driven stiction models with one or two parameters, whose structure is rather limited; as a result, data-driven stiction models may not be able to describe the actual complicated signatures of sticky control valves in

practice. For example, the input $u(t)$ and output $x(t)$ of an industrial control valve from a large-scale thermal power plant in China are measured with a sampling period of 0.5 s, with their time trends given in Figure 1 and the valve signature in
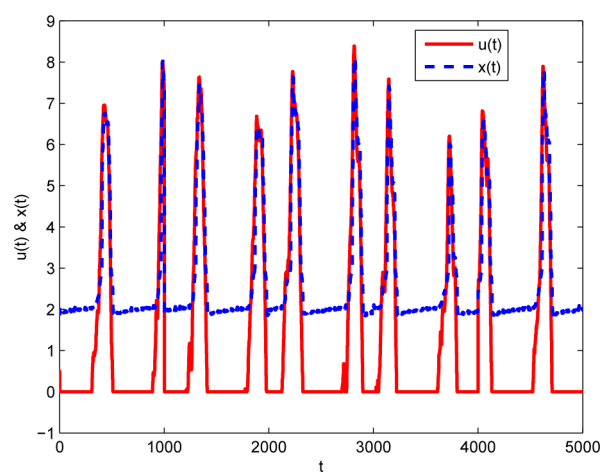

Figure 1. Input $u(t)$ (red −) and output $x(t)$ (blue - - -) of an industrial control valve.

Figure 2. It is clearly revealed from Figure 2 that this control valve exhibits complex behaviors beyond the data-driven stiction models used in the above articles. Such an observation motivates us to look for a control valve model with more flexible structure. In our earlier attempt,[17] two point-slope models are used to describe the ascend and descend paths of control valves, so that asymmetric control valve stiction can be captured. However, the identification method therein requires the signals in closed-control loop oscillating between two
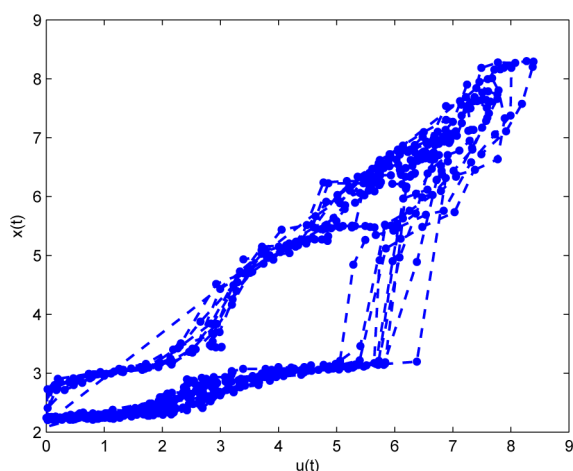
Figure 2. Signature plot of an industrial control valve.

extreme values. Such a requirement cannot be fulfilled when the closed-control loop experiences a set point variation and/or a load disturbance perturbation. Therefore, our objective is to have a flexible control valve model that can capture complex control valve signatures and can be identified under oscillatory or general types of input signals. It is also worthy to point out that some articles[18−25] studied the identification of Hammerstein systems with nonstatic input nonlinearities. However, a common feature of these works is the requirement of specially designed inputs; as a result, the proposed methods therein cannot be applied to oscillatory or general signals in closed-control loops, where the controller outputs, as the inputs of Hammerstein systems, are usually not subject to the users' design.

The contributions of this Article are 2-fold. First, we introduce Preisach model to describe sticky control valves as the input nonlinearity of Hammerstein system. Although Preisach model has been widely applied to model hysteresis phenomena in the fields of mechanics, magnetic, and smart materials,[26−28] the use of Preisach model to describe sticky control valves in this Article is a first attempt to the best of our knowledge. Different from the data-driven stiction models,[7−10,14] Preisach model can be regarded as a nonparametric model with many weighting parameters to be estimated, which is the fundamental reason that Preisach model is flexible enough to describe complicated signatures of sticky control valves. To avoid high variances, a common problem for models with higher flexibility,[29] a regularized iterative method is proposed to estimate the weighting parameters of discretized Preisach model and the parameters of linear dynamic subsystem. Second, because a known sufficient PE condition of general input signals is not satisfied by oscillatory signals, we establish the persistently exciting (PE) condition for oscillatory input signals in the identification of discretized Preisach models. With the established PE conditions, Hammerstein system using Preisach model as the input nonlinearity is identifiable. Under oscillatory input signals, Preisach model is proved to enclose the data-driven stiction models with one or two parameters, including Stenman's stiction model,[30] Choudhury's stiction model,[31] Kano's stiction model,[32] and He's stiction model.[33] Thus, with the proved relation between Preisach model and data-driven stiction models, Preisach model is eligible for sticky control valves that can be described by data-driven stiction models, and those having more complicated

signatures such as the one in Figure 2. Along with the flexibility of Preisach model for describing sticky control valves, a new issue concerning the stiction quantification arises: the Preisach model is nonparametric so that it does not have a stiction index to quantify the stiction severity, while data-driven stiction models have well-defined ones, for example, f_s and f_d for He's stiction model defined later in Figure 5. This issue is beyond the modeling topic of this Article and is thus not discussed herein.

A preliminary version of this study was presented as a conference paper;[34] this study provides new results on the regularized iterative identification method and on the relation between Preisach model and data-driven stiction models.

The rest of this Article is organized as follows. Section 2 formulates the identification problem for Hammerstein system. Section 3 shows the ability of Preisach model in capturing data-driven stiction models. Section 4 proposes the identification method. Section 5 establishes a PE condition for the oscillatory signals having only two extreme values. Section 6 provides simulated, experimental, and industrial examples. Some concluding remarks are given in section 7.

2. PROBLEM FORMULATION

Consider the Hammerstein system shown in Figure 3:

$$A(q^{-1})y(t) = B(q^{-1})x(t) + c + e(t) \tag{1}$$

$$x(t) = f(u(t)) \tag{2}$$

with

$$A(q^{-1}) = 1 + a_1 q^{-1} + \ldots + a_{n_a} q^{-n_a}$$

$$B(q^{-1}) = b_1 q^{-n_k-1} + \ldots + b_{n_b} a^{-n_k-n_b}$$

Here, $u(t)$, $y(t)$, $x(t)$, and $e(t)$ are the discrete-time input, output, inner input, and zero-mean white noise signals, respectively. The inner signal $x(t)$ and the noise $e(t)$ are not measurable. Symbol q^{-1} stands for one-sample delay operator, that is, $q^{-1}x(t) = x(t-1)$. Symbols $a \triangleq [a_1, \ldots, an_a]$, $b \triangleq [b_1, \ldots, bn_b]$, and c are the unknown real-valued parameters to be estimated. Symbols n_a and n_b are, respectively, the orders of $A(q^{-1})$ and $B(q^{-1})$, and n_k is the time delay of the linear subsystems; they are the integer-valued structure parameters to be determined too. With a temporary abuse of t as a continuous variable, the nonlinear block $f(\cdot)$ is described by Preisach model:[28,35]

$$f(t) = \iint_{(\beta,\alpha) \in P} \mu(\beta, \alpha) \gamma_{\beta\alpha}(t) \, d\beta \, d\alpha \tag{3}$$

Here, P stands for the so-called effective Preisach plane:

$$P \triangleq \{(\beta, \alpha) | \beta \geq u_{\min}, \alpha \leq u_{\max}, \beta \leq \alpha\}$$

where the range of $u(t)$ is denoted as $[u_{\min}, u_{\max}]$. The notation $\mu(\beta, \alpha)$ is a weighting function associated with the point $(\beta, \alpha) \in P$. The symbol $\gamma_{\beta\alpha}$ is the relay operator:

$$\gamma_{\beta\alpha}(t) = \begin{cases} +1, & \text{if } u(t) > \alpha \\ -1, & \text{if } u(t) < \beta \\ \gamma_{\beta\alpha}(t^-) \triangleq \lim_{t' < t, t' \to t} \gamma_{\beta\alpha}(t'), & \text{if } \beta \leq u(t) \leq \alpha \end{cases}$$

Preisach model in eq 3 can be regarded as a nonparametric model because it is a weighted superposition of infinite relay

operators $\gamma_{\beta\alpha}(t)$ with weighting parameters $\mu(\beta,\alpha)$. This nonparametric characteristic enables Preisach model to capture the complicated signatures of sticky control valves. If the threshold couple (β,α) is limited to the line $\beta = \alpha$, and the weighting function $\mu(\beta,\alpha)$ is an impulse function, then eq 3 can represent both continuous and discontinuous static nonlinearities. In particular, the relay and backlash can be easily proved to be special cases of Preisach model.[27] As a result, Preisach model is proper for hysteresis-type nonlinearities with memory effects as well as static nonlinearities, both of which are possibly encountered in control valves.
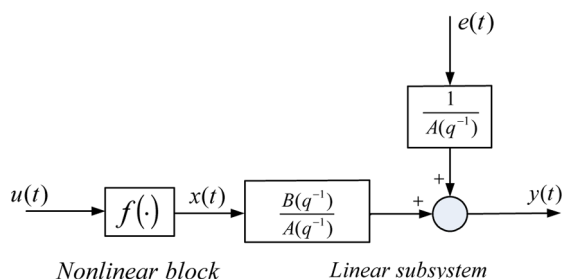

Figure 3. Diagram of Hammerstein system.

With the oscillatory or more general measurements $\{u(t),y(t)\}_{t=1}^{N}$, the identification objective is to estimate the unknown parameters of linear subsystem, a, b, and c, associated with the structure parameters (n_a, n_b, n_k), and the unknown Preisach model $f(\cdot)$.

3. PREISACH MODEL FOR STICKY CONTROL VALVES

This section recalls the types of nonlinearities that can be described by Preisach model, and establishes the relation between Preisach model and data-driven stiction models.

A natural question in using Preisach model to describe sticky control valves is: What kind of sticky control valves can be described by Preisach model? A direct answer is not available, but the question can be answered indirectly as follows: if the signature of sticky control valve satisfies the following wiping-out property, congruency property, and rate-independence property, then the control valve can be described by Preisach model. These three properties have been shown to a sufficient and necessary condition for hysteresis-type nonlinearities that can be represented by Preisach model.[28]

Property 1 (Wiping-Out Property[28]). Only the alternating series of dominant input extrema are stored by Preisach model; all other input extrema are wiped out (see eqs 5 and 6 in the proof of Proposition 1 for the definition of dominant input extrema).

Property 2 (Congruency Property[28]). All hysteresis loops corresponding to the same extreme values of input are congruent in the geometric sense (i.e., the loops are identical up to linear translation).

Property 3 (Rate-Independence Property[26]). The path of the input−output couple $(u(t), f(t))$ of the hysteresis nonlinearity is invariant with respective to any increasing time homeomorphism (i.e., the path is independent of the variation velocity of $u(t)$).

Next, we illustrate how these three properties are verified for a given signature of sticky control valve. As a model with more flexible structure, Preisach model will be proved to enclose the data-driven stiction models for sticky control valve in

oscillations, including Stenman's stiction model,[30] Choudhury's stiction model,[31] Kano's stiction model,[32] and He's stiction model.[33]

He's stiction model[33] is one of the well-accepted data-driven models for sticky control valves. The signature plot of He's stiction model is shown in Figure 4. The flowchart of He's
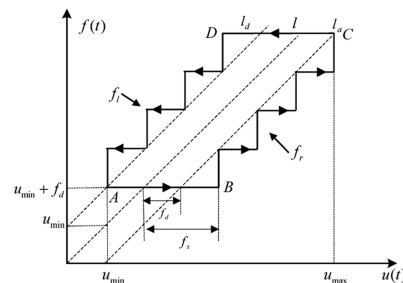

Figure 4. Signature plot of He's stiction model.
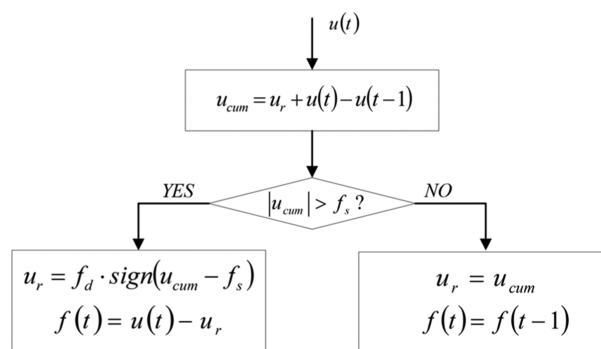

Figure 5. Flowchart of He's stiction model (adapted from Figure 2 in ref 33).

stiction model is reproduced in Figure 5 (note that the stiction model is in the discrete time so that $u(t-1)$ and $u(t)$ represent two consecutive samples of input). The parameters f_s and f_d in Figure 5 stand for the static and kinetic friction bands, respectively. The variables u_r and u_{cum} are the residual and cumulative forces acting on the valve, respectively.

Proposition 1: He's stiction model in Figure 5 can be described by Preisach model.

Proof: Suppose that the range of the input $u(t)$ is $[u_{min}, u_{max}]$ satisfying $u_{max} - u_{min} > f_s + f_d$, and the input is equal to u_{min} at the initial time instant $t = 0$. Denote the limiting descend branch CDA and ascend branch ABC in Figure 4 as f_l and f_r, respectively. The curves f_l and f_r have finite number of output values f_i, $i = 1, 2, ..., i_{max}$, which is defined as

$$f_i = u_{min} + if_d, \ i = 1, 2, ..., i_{max} \triangleq \left\lfloor \frac{u_{max} - u_{min} - 2f_d}{f_s - f_d} \right\rfloor$$

(4)

where the symbol $\lfloor \cdot \rfloor$ is the largest integer less than or equal to the operand.

We need to prove that He's stiction model satisfies the three properties, the wiping-out property, the congruency property, and the rate-independence property.

First, Property 1 (wiping-out property) is proved to be satisfied by inductive reasoning as follows. For a general input

variation $u(t)$ with $0 \leq t \leq t'$, the dominant input maximum M_k and the dominant input minimum m_k for a positive integer k are defined, respectively, as

$$M_k = \max_{t \in [t_{k-1}^-, t']} u(t), \quad u(t_k^+) = M_k \tag{5}$$

$$m_k = \min_{t \in [t_k^+, t']} u(t), \quad u(t_k^-) = m_k \tag{6}$$

with $t_0^- \triangleq 0$. Figure 6 shows an illustrative example of $u(t)$, M_k, and m_k. From the signature plot and flowchart of He's stiction
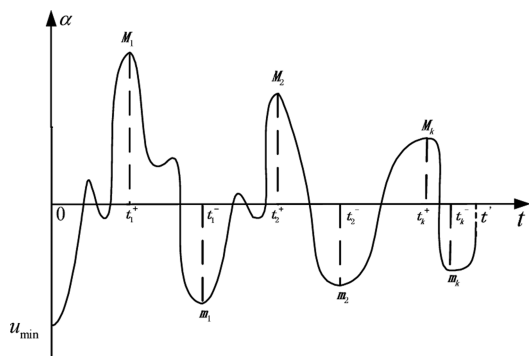

Figure 6. Input for the proof of Proposition 1.

model, respectively, shown in Figures 4 and 5, only two cases may occur for M_1:

- In the case of $M_1 \in [u_{\min}, u_{\min} + f_d + f_s]$, $u(t)$ for $t \in [0, t']$ always gives a constant output equal to $u_{\min} + f_d$. Thus, all of the previous local input extrema for $t < t_1^+$ are wiped out by M_1.
- In the case of $M_1 \in (u_{\min} + f_d + f_s, u_{\max}]$, the output is finally increased along the right discontinuous border f_r to some f_i defined in eq 4, denoted as $f_{i_1^+}$ here, no matter what the input path for $t \in [0, t_1^+]$ is. The flowchart of He's stiction model in Figure 5 says in this case the previous local input extrema for $t < t_1^+$ do not affect the output after the time instant $t = t_1^+$. That is, the previous input extrema are wiped out by this maximum M_1.

Similarly, two cases need to be discussed for the dominant input minimum m_1:

- In the case of $m_1 \in [f_{i_1^+} - f_s, M_1]$ with $M_1 \in (u_{\min} + f_d + f_s, u_{\max}]$, the output moves in the inner horizontal line connecting the two borders f_l and f_r. The input for $t \in$

$[t_1^+, t']$ always gives a constant output value equal to $f_{i_1^+}$. Thus, the wiping-out property always holds.

- In the case of $m_1 \in [u_{\min}, f_{i_1^+} - f_s)$, the input is finally decreased along the left border f_l to some $f_{i_1^-}$, starting from time instant t_1^+. The flowchart of He's stiction model in Figure 5 then says that the previous local input extrema for $t \in [t_1^+, t']$ do not affect the output after the time instant $t = t_1^-$. That is, the previous local input extrema in $[t_1^+, t_1^-]$ are wiped out by this minimum m_1.

Analogously to M_1 and m_1, the other dominant input extreme series $\{M_2, M_3, ...\}$ and $\{m_2, m_3, ...\}$ wipe out all of the intermediate local input extreme values that appeared before the time instants t_k^+ and t_k^-, respectively. Therefore, the wiping-out property holds for He's stiction model.

Next, Property 2 (congruency property) is proved. When the input $u(t)$ oscillates between two extreme values, the minimum u_1 and the maximum u_2, with different initial outputs x_1 and x_2, respectively, only two cases form the hysteresis loop, shown in Figure 7:

(a) In the case that the input oscillates between the left and right borders, no matter what the initial outputs are, the corresponding hysteresis loops are degenerated to horizontal lines, shown as the thick solid lines in Figure 7 (left), which are congruent in the geometric sense.

(b) In the case that the input interval $[u_1, u_2]$ is large enough, the output is increased along the right border to the local maximum f_i and decreased along the left border to the local minimum f_j defined in eq 4. Thus, only one hysteresis loop is formed, shown as the thick solid lines in Figure 7 (right), and the congruency property certainly holds.

Because He's stiction model in Figure 5, which is clearly rate-independent, satisfies the wiping-out property and congruency property, it can be described by Preisach model.

Proposition 1 proves that Preisach model can describe He's stiction model as a special case. A related question is what is the weighting function $\mu(\beta, \alpha)$ for this model? Mayergoyz[28] proposed one method based on the so-called first-order reversal functions to calculate $\mu(\beta, \alpha)$. Using this method, we obtain the weighting function $\mu(\beta, \alpha)$ for He's stiction model with parameters f_s and f_d, as a Delta function sequence located at some specific points along the line $\alpha = \beta + f_d + f_s$ on the Preisach plane:
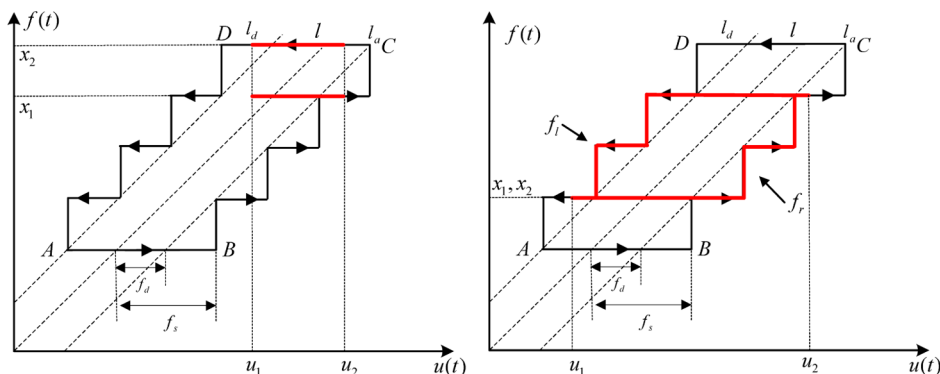

Figure 7. Signature plots generated from the small-amplitude (left) or large-amplitude (right) input variation for the proof of congruency property in Proposition 1.

D

$$\mu(\beta, \alpha) = \frac{f_s - f_d}{2} \sum_{j=1}^{j_{max}} \delta(\beta - \beta_j, \alpha - \alpha_j) \tag{7}$$

Here, the two-dimensional Delta function $\delta(\beta - \beta_j, \alpha - \alpha_j)$ is defined as

$$\delta(\beta - \beta_j, \alpha - \alpha_j) = 0, \ \forall \ (\beta, \alpha) \neq (\beta_j, \alpha_j),$$

$$\text{and} \int_{-\infty}^{\infty} \int_{-\infty}^{\infty} \delta(\beta - \beta_j, \alpha - \alpha_j) \, d\beta \, d\alpha = 1,$$

$$\alpha_j = u_{min} + f_d + j(f_s - f_d), \text{ and } \beta_j = \alpha_j - (f_s + f_d),$$

$$j = 1, 2, ..., j_{max} \triangleq \left\lfloor \frac{u_{max} - u_{min} - f_s - f_d}{f_s - f_d} \right\rfloor \tag{8}$$

Analogously to the proof of Proposition 1, Preisach model can be proved to enclose the other data-driven stiction models for describing the behaviors of sticky control valve in oscillations, including Stenman's stiction model,[30] Choudhury's stiction model,[31] and Kano's stiction model.[32]

Proposition 2: Under oscillatory types of input signals, Stenman's stiction model, Choudhury's stiction model, and Kano's stiction model can be described by Preisach model.

4. IDENTIFICATION METHOD

This section presents a regularized iterative method for identification of Hammerstein system.

Preisach model in eq 3 has to be discretized for identification purpose. The discretized Preisach model is[36−38]

$$f(t) = \sum_{i=1}^{L} \sum_{j=i}^{L} \mu_{ij} \gamma_{ij}(t) \tag{9}$$

where μ_{ij} is the weighting parameter and $\gamma_{ij}(t)$ is the discretized relay operator:

$$\gamma_{ij}(t) = \begin{cases} +1, & \text{if } u(t) < (u_j + u_j + 1)/2 \\ -1, & \text{if } u(t) < (u_i + u_i + 1)/2 \\ \gamma_{ij}(t-1), & \text{otherwise} \end{cases} \tag{10}$$

Here, u_i (or u_j) is the discretized threshold:

$$u_i = u_{min} + (i - 1)\delta, \ i = 1, 2, ..., L + 1 \tag{11}$$

where L is the discretization level and δ is the discretization step size:

$$\delta = \frac{u_{max} - u_{min}}{L} \tag{12}$$

The connection between discretized Preisach model and its continuous counterpart was established by Theorem 4.1 in Banks et al.[36] It states that, as the discretization level L approaches infinity, the output of discretized Preisach model in eq 9 converges to its continuous counterpart in eq 3.

The discretized Preisach model in eq 9 can be rewritten in a compact form:

$$f(t) = \gamma^T(t)\mu \tag{13}$$

where

$$\mu \triangleq [\mu_1, ..., \mu_K]^T \triangleq [\mu_{11}, ..., \mu_{1L}, \mu_{22}, ..., \mu_{2L}, ..., \mu_{LL}]^T \tag{14}$$

and

$$\gamma(t) \triangleq [\gamma_1(t), ..., \gamma_K(t)]^T$$
$$\triangleq [\gamma_{11}(t), ..., \gamma_{1L}(t), \gamma_{22}(t), ..., \gamma_{2L}(t), ..., \gamma_{LL}(t)]^T \tag{15}$$

with the length of the vectors μ and $\gamma(t)$ equal to $K \triangleq L(L + 1)/2$. Substituting eq 13 into eq 1 yields

$$y(t) = -\phi^T(t)a + b^T\Gamma(t)\mu + c + e(t)$$

where

$$\phi(t) = [y(t - 1), ..., y(t - n_a)]^T$$

$$\Gamma(t) = \begin{bmatrix} \gamma_1(u(t - n_k - 1)) & \cdots & \gamma_K(u(t - n_k - 1)) \\ \vdots & \ddots & \vdots \\ \gamma_1(u(t - n_k - n_b)) & \cdots & \gamma_K(u(t - n_k - n_b)) \end{bmatrix}$$

Define the loss function for parameters estimate as

$$J_N(a, b, c, \mu) = \sum_{t=1}^{N} (y(t) + \phi^T(t)a - b^T\Gamma(t)\mu - c)^2 \tag{16}$$

On the basis of the measurements $\{u(t), y(t)\}_{t=1}^{N}$, and the user-selected upper limits of n_a, n_b, n_k, and L, denoted, respectively, as $n_{a,U}$, $n_{b,U}$, $n_{k,U}$, and L_U, we propose a regularized iterative method to determine the structure parameters (n_a, n_b, n_k) and the discretization level L in an outer loop, and calculate the parameter vectors a, b, c, and μ iteratively in an inner loop. The proposed method consists of the following steps:

Outer loop for $\hat{n}_a = 1: n_{a,U}$, $\hat{n}_b = 1: n_{b,U}$, $\hat{n}_k = 0: n_{k,U}$, and $\hat{L} = 2: L_U$.

Step A: Estimate a, b, c, and μ in the following inner loop using $\hat{n}_a$, $\hat{n}_b$, $\hat{n}_k$, and $\hat{L}$.

Inner loop for $k = 1, 2, ...$ until convergence.

Step 1: Select the initial estimates as

$$\hat{a}(0) = [0, 0, ..., 0]^T, \ \hat{b}(0) = [1, 0, ..., 0]^T, \ \hat{c}(0) = 0$$

Step 2: Estimate the parameter μ of discretized Preisach model at the kth iteration $(k = 1, 2, ...)$ by solving a regularized nonnegative linear least-squares constraint problem as

$$\bar{\mu}(k) = \arg\min_{\mu} J_N(\hat{a}(k - 1), \hat{b}(k - 1), \hat{c}(k - 1), \mu),$$

$$\text{s.t., } \mu \geq 0, \ \|\mu\|_1 \triangleq \sum_{i=1}^{K} |\mu_i| \leq \eta \tag{17}$$

where η is the regularization parameter, and $\hat{a}(k - 1)$, $\hat{b}(k - 1)$, and $\hat{c}(k - 1)$ are the estimates of a, b, and c in the $(k - 1)$th iteration, respectively.

Step 3: Update the estimates of a, b, and c of the linear subsystem by solving a linear least-squares problem:

$$\{\bar{a}(k), \bar{b}(k), \bar{c}(k)\} = \arg\min_{a,b,c} J_N(a, b, c, \bar{\mu}(k)) \tag{18}$$

Step 4: Normalize the above estimates as

$$\hat{\mu}(k) = s(k)\bar{\mu}(k)\| \bar{b}(k)\|, \ \hat{b}(k) = \frac{s(k)}{\| b(k)\|}\bar{b}(k),$$

$$\hat{a}(k) = \bar{a}(k), \ \hat{c}(k) = \bar{c}(k) \tag{19}$$

where $s(k)$ is the sign of the first nonzero element of $\bar{b}(k)$, and $\|\cdot\|$ stands for the Euclidean norm of the operand.

Step 5: Design a convergence criterion to monitor the relative percentage improvement of the estimated parameters:

$$\frac{\|\hat{\vartheta}(k) - \hat{\vartheta}(k-1)\|}{\|\hat{\vartheta}(k)\|} < \zeta$$

where $\hat{\vartheta}(k)$ stands for the estimated parameter vector composed by $\hat{a}(k)$, $\hat{b}(k)$, $\hat{c}(k)$, and $\hat{\mu}(k)$, and ζ is a small positive real number close to zero, for example, $\zeta = 0.01$. Stop the iteration if the estimated parameters satisfy the convergence criterion; otherwise, set $k = k + 1$ and go to step 2.

End of Inner Loop. Step B: On the basis of the estimated parameter vectors $\hat{a}$, $\hat{b}$, $\hat{c}$, and $\hat{\mu}$ from the inner loop, calculate the fitness between the measured output $y(t)$ and simulated output $\hat{y}_s(t)$:

$$F(\hat{n}_a, \hat{n}_b, \hat{n}_k, \hat{L}) = \left(1 - \frac{\|\hat{y}_s(t) - y(t)\|}{\|y(t) - E\{y(t)\}\|}\right) \times 100\%$$

(20)

where

$$\hat{y}_s(t) = \frac{\sum_{j=1}^{\hat{n}_b} \hat{b}_j q^{-j}}{1 + \sum_{i=1}^{\hat{n}_a} \hat{a}_i q^{-i}} \gamma^T(u(t - \hat{n}_k))\hat{\mu} + \frac{1}{1 + \sum_{i=1}^{\hat{n}_a} \hat{a}_i q^{-i}} \hat{c}$$

and $E\{\cdot\}$ stands for the mean value of the operand.

Step C: If the fitness $F(\hat{n}_a, \hat{n}_b, \hat{n}_k, \hat{L})$ is larger than the counterpart in the previous iteration, then preserve the estimated parameter vectors $\hat{a}$, $\hat{b}$, $\hat{c}$, and $\hat{\mu}$; otherwise, discard these estimated parameter vectors. Next, go back to step A until the completion of the grid search on the structure parameters $\hat{n}_a$, $\hat{n}_b$, $\hat{n}_k$, and $\hat{L}$.

End of Outer Loop. The discretized Preisach model is used to describe the behavior of sticky control valves whose output is always nondecreasing when the input increases. To meet with this physical fact, a constraint $\mu \geq 0$ is incorporated into the above step 2. In addition, as a nonparametric model with high flexibility, many weighting parameters of discretized Preisach model may be close to zero due to the noise effects in data samples. To avoid high variances, the main idea of a regularization technique for linear system identification, the Least Absolute Selection and Shrinkage Operator (LASSO),[39] is borrowed to formulate the optimization problem in eq 17. In particular, the regularization parameters η in eq 17 can be selected as

$$\eta = \kappa \|\mu_{\text{NLS}}(k)\|_1$$

(21)

where $\mu_{\text{NLS}}(k)$ is the estimate of eq 17 with $\kappa = 1$, for which the L_1-norm constraint plays no role. To have a better trade-off between the model bias and variance, the well-known Bayesian Information Criterion[40] (BIC) is used here to determine optimal regularization parameters η in a preselected interval $\kappa \in [0.95, 1]$:

$$\text{BIC}(\kappa) = N \log \hat{\sigma}^2 + P \log N$$

(22)

where $\hat{\sigma}^2$ is the variance of the residual of the estimated model $\{y(t) - \hat{y}_s(t)\}_{t=1}^N$, and P is the total parameter length $n_a + n_b + n_k + K_0$, with K_0 being the number of nonzero weighting parameter μ_i.

The computational cost of the proposed method is acceptable for practical applications. The outer loop is a grid search for integer-valued structure parameters n_a, n_b, n_k, and L, and is a standard identification step. The computation in the

inner loop is in the same principle as the iterative method for convectional Hammerstein systems, which usually takes very few steps for convergence.[41] In addition, the inner loop is composed by two linear least-squares optimization problems in eqs 17 and 18 that can be solved efficiently. The computational time in each least-squares optimization mainly depends on the data length N and the sizes of parameter vectors a, b, and μ. Note that the size K of μ in eq 14 has a quadratic relation with the discretization level L, that is, $K = L(L + 1)/2$. These statements are numerically illustrated in Example 3 later.

5. PERSISTENTLY EXCITING CONDITIONS

This section studies the PE conditions for oscillatory and general types of input signals.

For the regularized iterative method in section 4, the linear subsystem and the input nonlinearity (the discretized Preisach model) are identified iteratively. The PE condition for the linear subsystem has been well established.[42] In brief, the inner signal $x(t)$ needs to have sufficient frequency components. This is usually satisfied, because $x(t)$ in the presence of control valve stiction is in the shape of rectangular waves or experiences multiple-step variation. Thus, we only need to investigate the PE condition for the discretized Preisach model. The question to be answered is: Are the oscillatory or general types of input signals informative enough to reach the true weighting parameter vector μ defined in eq 14?

We revisit one sufficient (but unnecessary) PE condition of a general input signal for identification of the discretized Preisach model established by Tan and Baras.[43] To ease the understanding of this condition, we introduce $\tilde{u}(t)$, referred to as the virtual input, which is obtained by rounding $u(t)$ to the nearest discretized threshold u_i in eq 11, that is:

$$\tilde{u}(t) = \begin{cases} u_{L+1}, & \text{if } u(t) > \frac{1}{2}(u_L + u_{L+1}) \\ u_i, & \text{if } \frac{1}{2}(u_{i-1} + u_i) < u(t) \leq \frac{1}{2}(u_i + u_{i+1}), \\ & \text{for } i = 2, ..., L - 1 \\ u_1, & \text{if } u(t) \leq \frac{1}{2}(u_1 + u_2) \end{cases}$$

(23)

For two different inputs, if they share the same virtual input $\tilde{u}(t)$, then the outputs of the discretized Preisach model in eq 13 are the same at all time instants.

Lemma 1: For the discretized Preisach model in eq 13 and the relay vector $\gamma(t)$ in eq 15, the difference sequence

$$\gamma_d(t) \triangleq \gamma(t) - \gamma(t-1)$$

(24)

is PE, if there exists a positive integer M, such that for any t_0 one can find a sequence $\{u'(t)\}_{t=t0}^{t0+M-1}$ belonging to the PE equivalence class (see section III-B and Figure 5 in ref 43 for the definition of PE equivalence class and an illustrative example) $\{u(t)\}_{t=t0}^{t0+M-1}$ of $u(t)$, where $\{u'(t)\}_{t=t0}^{t0+M-1}$ satisfies the following conditions:

(a) The discretized thresholds u_i's for $i = 1, 2, ..., L + 1$ (defined in eq 11) are covered by local maxima and local minima of the virtual input signal $\tilde{u}'(t)$ in eq 23.

(b) Two local maxima (minima) of $\tilde{u}'(t)$ adjacent in time index t differ from each other by no more than one discretization step size δ in eq 12.

(c) The series of local maxima of $\tilde{u}'(t)$ is nonincreasing (nondecreasing), and the series of local minima is nondecreasing (nonincreasing).

Lemma 1 can be used to investigate whether oscillatory signals satisfy the PE condition. Consider the case that the input $u(t)$ varies between two extreme values $u_{\min}$ and $u_{\max}$ with $u_{\min} < u_{\max}$. According to Lemma 1, if the discretization level L is greater than 2, then the oscillatory input $u(t)$ with only two extrema is not PE. However, L is usually much larger than 2 in practice, which leads to a conclusion that the oscillatory input does not satisfy the PE condition in Lemma 1. Hence, we need to establish a relaxed version of Lemma 1 for inputs being oscillatory with only two extrema so that the oscillatory signals are informative for identification of discretized Preisach model.

Proposition 3: If the discretization level of the discretized Preisach model in eq 9 is L, and the virtual input signal $\tilde{u}(t)$ in eq 23 being oscillatory with only two extrema varies no more than one discretization step size δ in 12, that is, $\tilde{u}(t)$ holds or changes from u_i to u_{i+1} or u_{i-1} (defined in eq 11) between two consecutive samples, then the discretized Preisach model using $2L - 1$ parameters is identifiable.

Proof: Let us extract some consecutive samples of $\{u(t)\}$ as a sequence $\{u(t)\}_{t=t_0}^{t_0+N-1}$ such that the sequence covers a full cycle of the active hysteresis loop. Without loss of generality, $\{u(t)\}_{t=t_0}^{t_0+N-1}$ starts from $u(t_0) = u_{\min}$ to $u(t_1) = u_{\max}$ for some time instant $t_1 \in (t_0, t_0 + N - 1)$ and goes back to $u(t_0 + N - 1) = u_{\min}$. In the time interval $t \in [t_0, t_1]$, the virtual input $\tilde{u}(t)$ holds or varies from u_j to u_{j+1}. If $\tilde{u}(t - 1) = u_j$ and $\tilde{u}(t) = u_{j+1}$ with the discretized threshold u_j defined in eq 11, then only the relay operators associated with μ_{ij}, $i = 1, ..., j$, give the outputs -1 at the time instant $(t - 1)$, and $+1$ at the time instant t, and other relay operators keep their outputs the same as the ones at the time instant $(t - 1)$, so that we have

$$f(u(t)) - f(u(t - 1)) = 2 \sum_{i=1}^{j} \mu_{ij} \tag{25}$$

Thus, $\mu_{\beta j} \triangleq \sum_{i=1}^{j}$ for $j = 1, 2, ..., L$ can be uniquely determined from eq 25. Similarly, in the time interval $t \in [t_1, t_0 + N - 1]$, the input $u(t)$ decreases no more than one level l between consecutive samples. If $\tilde{u}(t - 1) = u_{i+1}$ and $\tilde{u}(t) = u_i$, then the output of the discretized Preisach model changes its value as

$$f(u(t)) - f(u(t - 1)) = -2 \sum_{j=i}^{L} \mu_{ij}$$

from which $\mu_{i\alpha} \triangleq \sum_{j=1}^{L} \mu_{ij}$ for $i = 1, 2, ..., L$ can be uniquely determined. Moreover, it is clear that $\sum_{i=1}^{L} \mu_{i\alpha} = \sum_{j=1}^{L} \mu_{\beta j} = (\mu_{\max} - \mu_{\min})/2$; therefore, there exists one redundant parameter, say, $\mu_{L\alpha}$. The single hysteresis loop in active then can be completely described by the parameters $\mu_{i\alpha}$ for $i = 1, 2, ..., L - 1$ and $\mu_{\beta j}$ for $j = 1, 2, ..., L$, and the oscillatory input $u(t)$ is sufficient to yield unique estimates of these $2L - 1$ parameters.

With the PE condition in Lemma 1 and the one established in Proposition 3, we are ready to identify Hammerstein system with discretized Preisach model as the input nonlinearity, based on oscillatory or general types of input signals.

6. EXAMPLES

This section presents examples to illustrate the applicability of Hammerstein system using Preisach model as the input nonlinearity and the effectiveness of the proposed identification method.

Example 1. This example is to demonstrate that He's stiction model can be described by the Preisach model, as stated in Proposition 1. A closed-loop simulation experiment is performed in the same configuration as an experimental case study for control valve stiction compensation.[44] That is, the proportional-integral (PI) controller is $C(s) = 0.25(1 + (1/50s))$, the process model is $\hat{G}(s) = ((3.8163)/(156.46s + 1)) e^{-2.5s}$, the parameters for He's stiction model are $\hat{f}_s = 8.4$, $\hat{f}_d = 3.5243$, and the sampling period is 0.5 s. The set point $r(t)$, controller output $u(t)$, valve position $x(t)$ (only for the purpose of validation), and process output $y(t)$ are measured and plotted in Figure 8. The regularized iterative method is applied,
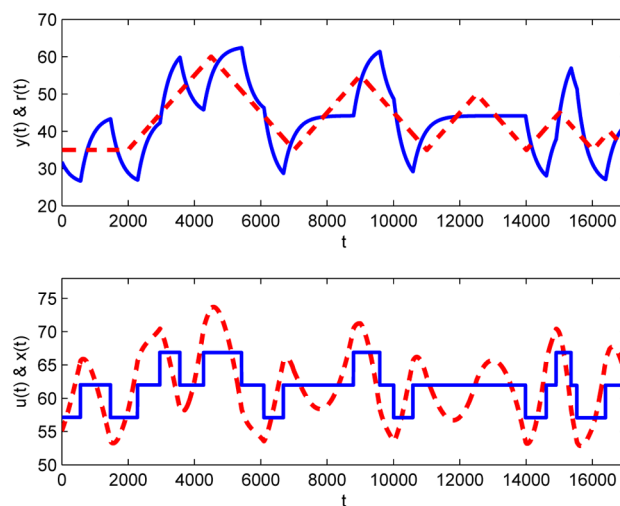

Figure 8. Set point $r(t)$ (upper, red - - -), process output $y(t)$ (upper, blue —), controller output $u(t)$ (lower, red - - -), and valve position $x(t)$ (lower, blue —) for Example 1.

and the optimal structure parameters are $\hat{n}_a = \hat{n}_b = 1$, $\hat{n}_k = 5$, and $\hat{L} = 16$. As shown in Figure 9, the estimated Preisach model fits very well with the actual He's stiction model, and the bode plots of the estimated and actual linear subsystems are almost overlapped to each other. The simulated output $\hat{y}_s(t)$ is compared to the measured one $y(t)$ in Figure 10. The fitness in 20 between $y(t)$ and $\hat{y}_s(t)$ is equal to 94.6871%. These results support Proposition 1 and prove the effectiveness of the regularized iterative method.

Example 2. This example is to reveal that Preisach model can describe the complicated sticky control valve shown in Figure 2, for which the data-driven stiction models in literature fail. Because the valve position $x(t)$ is accessible for this control valve, the linear subsystem of Hammerstein system is set to be unit. The regularized iterative method is applied to the measurements $\{\mu(t), x(t)\}_{t=1}^{5000}$ in Figure 1. The optimal structure parameters are determined as $\hat{L} = 20$. The estimated signature is given in the left subfigure of Figure 11. The left subfigure of Figure 12 compares the measured output $x(t)$ and estimated one $\hat{x}_s(t)$, where the fitness between $x(t)$ and $\hat{x}_s(t)$ is equal to 88.6555%.

As comparison, He's and Kano's stiction models are used to describe this control valve. By following the identification approach proposed by Jelali,[8] grid search methods are exploited to obtain the optimal estimates of the stiction parameters f_s and f_d of He's stiction model, and the counterparts S and J of Kano's stiction model, by achieving the largest fitness between $x(t)$ and its estimate. The stiction parameters are estimated to be $\hat{f}_s =$
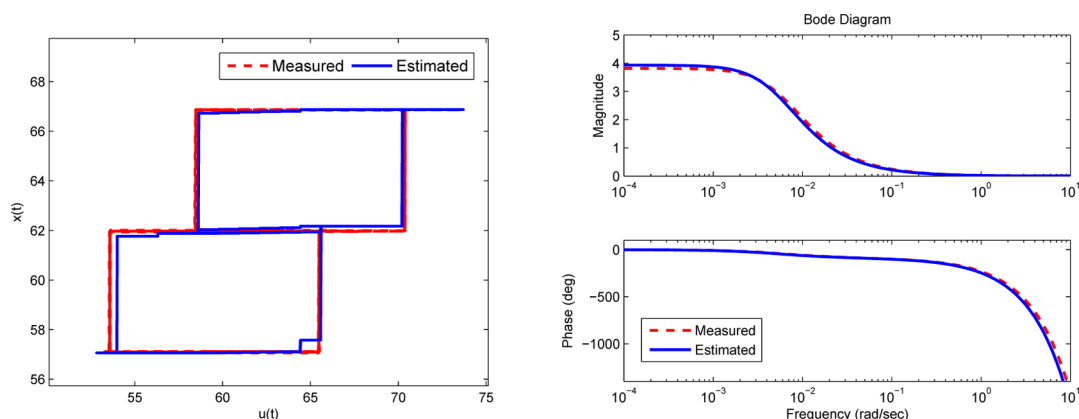
Figure 9. Valve signatures (left) and the bode plots (right) from the actual Hammerstein system (red - - -) and the estimated one (blue —) for Example 1.
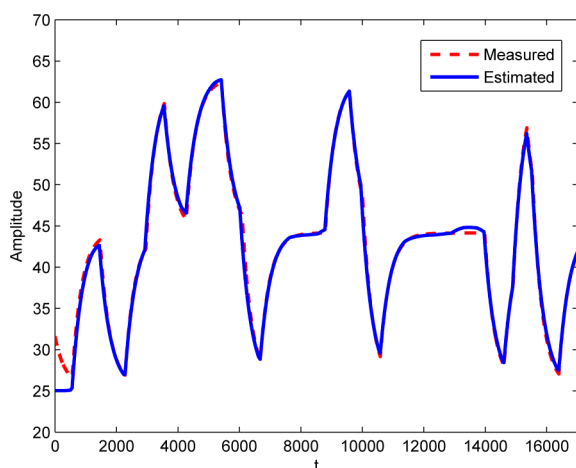

Figure 10. Measured output (red - - -) and the simulated output (blue —) for Example 1.

2.5812, $\hat{f}_d = 0$ for He's stiction model, and $\hat{S} = 4.3021$, $\hat{J} = 0.4302$ for Kano's stiction model. The estimated control valve stiction for He's stiction model is presented in the middle subfigure of Figure 11 with the output fitness 62.3160%, and the one for Kano's stiction model is in the right subfigure of Figure 11 with the output fitness 63.1789%. The middle and right subfigures of Figure 12 compare the measured output $x(t)$ and estimated ones $\hat{x}_s(t)$ from the two models. It is clear that Preisach model performs much better than the two data-driven stiction models, which supports the usage of Preisach model in describing sticky control valves in practice.

Some issues may need to be clarified for the unsatisfactory performance of He's and Kano's stiction models. First, the piecewise saturation of $u(t)$ and $x(t)$, as shown in Figure 1, is not one of the culprits, because He's and Kano's stiction models can handle saturated signals. Figure 12 clearly shows that when $x(t)$ is piecewise saturated, the outputs from Preisach model, He's and Kano's stiction models are also piecewise saturated, which is consistent with the actual valve signature in Figure 2. Second, the stiction is a character of valve body, not related to whether a pneumatic or electric valve actuator is used. The signatures of sticky pneumatic and electric valves are the same, so that the type of control actuators is also not the cause leading to the unsatisfactory performance of He's and Kano's stiction model. Third, the valve position $x(t)$ here is measured by a valve positioner, which works in the open-loop condition. This fact can be revealed by observing the signature plot of the control valve in Figure 2. That is, if there exists a feedback control loop in the valve positioner, the signature plot should exhibit smooth movements due to the dynamics of the positioner feedback control loop, instead of the straight lines formulating jumpy characters shown in Figure 2. By excluding the above three issues, we may conclude that He's and Kano's stiction models perform unsatisfactorily, mainly because the control valve suffers from seriously asymmetric stiction nonlinearity shown in Figure 2; the stiction of this industrial control valve is severe around the opening position, but the stiction is relatively minor in other positions.

Example 3. This example is to show that oscillatory signals satisfy the PE condition as proved in Proposition 3, and Preisach model encloses the data-driven stiction models as special cases. An industrial feedback control loop labeled *cdata.chemicals.loop23* in the database (http://www.ualberta.ca/
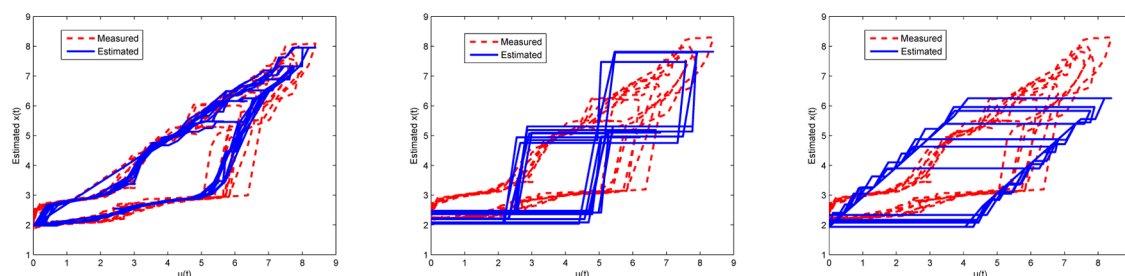

Figure 11. Measured signature (red - - -) and the estimated signatures (blue —) from Preisach model (left), He's stiction model (middle), and Kano's stiction model (right) for Example 2.
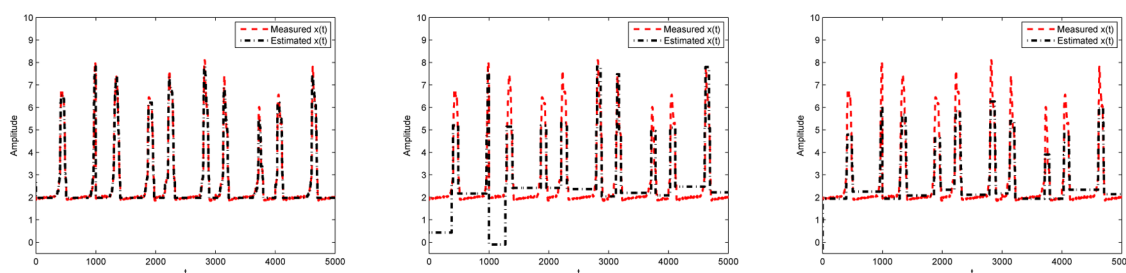
Figure 12. Comparison between $x(t)$ (red - - -) and its estimate $\hat{x}(t)$ (- · - · -) from Preisach model (left), He's stiction model (middle), and Kano's stiction model (right) for Example 2.

~bhuang/Stiction-Book.htm) accompanied by the book[4] is investigated here. The measurements of input $u(t)$ and output $y(t)$ are shown in Figure 13, which clearly shows that the input
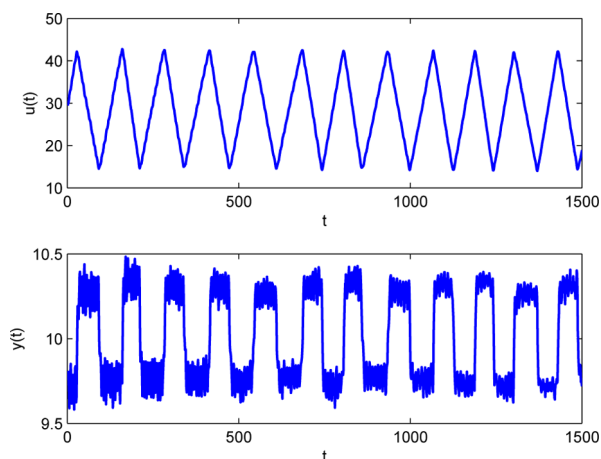

Figure 13. Input $u(t)$ and output $y(t)$ of an industrial feedback control loop for Example 3.

$u(t)$ is oscillatory with two extreme values. The sampling period is 10 s. As commented by the data provider (Dr. C. Scali), the control valve is (likely) with stiction, while the actual valve position is not available.

The proposed regularized iterative method is applied to the collected data $\{u(t), y(t)\}_{t=1}^{1500}$ in Figure 13. The estimated input nonlinearity and the bode plot of estimated linear subsystem are shown in Figure 14, with optimal structure parameters $\hat{n}_a = \hat{n}_b = 1$, $\hat{n}_k = 0$, and $\hat{L} = 14$. The fitness in eq 20 between the
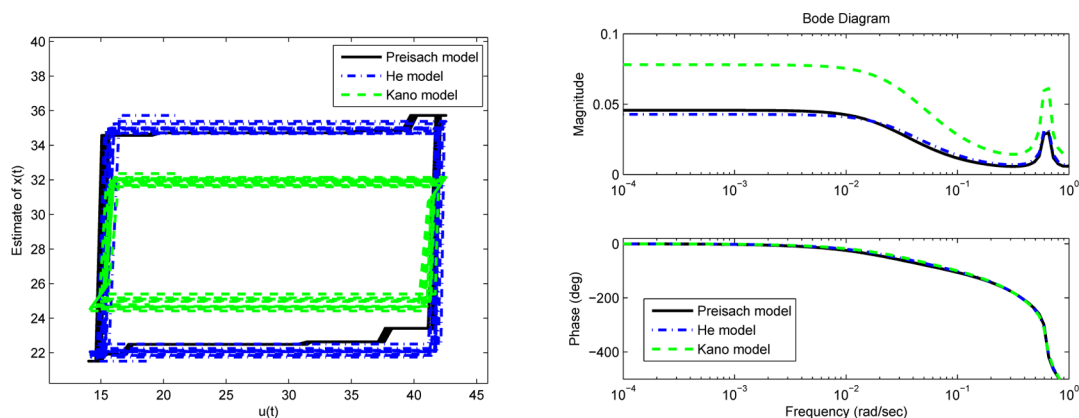
measured output $y(t)$ and the simulated one $\hat{y}_s(t)$ is 76.8699%, and as shown in Figure 15, $\hat{y}_s(t)$ can well capture the main

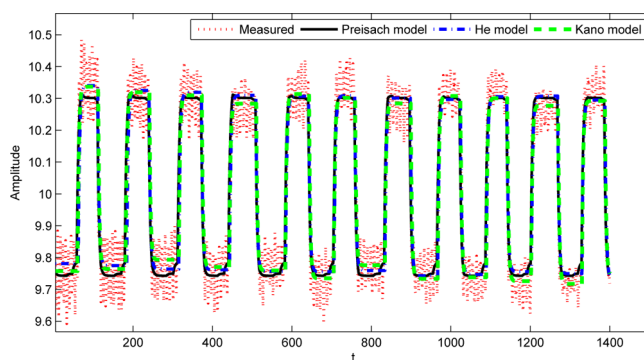**Figure 15.** Measured output $y(t)$ (red · · ·), simulated output $\hat{y}_s(t)$ (−) of Hammerstein system using Preisach model as the input non-linearity, simulated output $\hat{y}_H(t)$ (blue - · - · -) of Hammerstein system using He's stiction model, and simulated output $\hat{y}_K(t)$ (green - - -) of Hammerstein system using Kano's stiction model for Example 3.

dynamic variations of $y(t)$. As a comparison, if He's and Kano's stiction models are used, the identified models are shown in Figure 14 as well. The stiction parameters are $\hat{f}_s = 19.5918$, $\hat{f}_d = 6.9388$ for He's stiction model, together with structure parameters of linear subsystems as $\hat{n}_a = \hat{n}_b = \hat{n}_k = 1$. For Kano's stiction model, $\hat{S} = 26.8$, $\hat{j} = 6.0$, $\hat{n}_a = \hat{n}_b = 1$, and $\hat{n}_k = 0$. The simulated outputs are also shown in Figure 15. The output fitness values for He's and Kano's stiction models are, respectively, equal to 77.5265% and 78.4522%. The estimated input nonlinearities and linear subsystems (except for a gain

Figure 14. Estimated input nonlinearities (left) and the bode plots of the estimated linear subsystem (right) of Hammerstein systems using Preisach model (−), He's stiction model (blue - · - · -), and Kano's stiction model (green - - -) as input nonlinearities for Example 3.

ambiguity between two blocks) in Figure 14 are very similar, which support the relation between Preisach model and data-driven stiction models established in Propositions 1 and 2, and the PE condition of oscillatory signals in Proposition 3.

Let us analyze the computational cost of the proposed regularized iterative method. The average computational time of the proposed method is calculated with different values of L and the same setting for structure parameters, $n_{a,U} = 3$, $n_{b,U} = 3$, $n_{k,U} = 10$. The results, based on a computer with Intel Core I5-2450 CPU (2.5G Hz) and 8 GB memory, are shown in Figure 16. As comparison, the counterparts for the Hammerstein
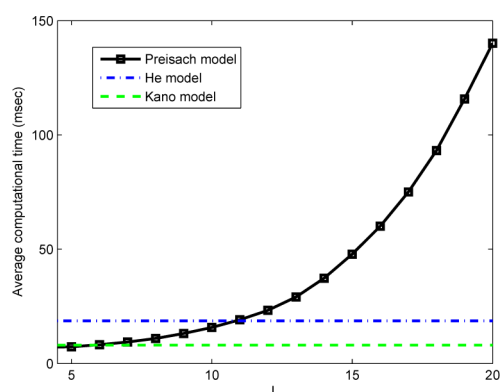

Figure 16. Average computational times of the proposed method (—) and the methods based on He's stiction model (blue - · - · -) and Kano's stiction model (green - - -) for Example 3.

systems with He's and Kano's stiction models are also given in Figure 16. It is clear that the proposed method has comparable efficiency when L is less than 10, and, as expected, the computational time quadratically increases with respect to the discretization level L. The average computation time for $L = 20$ is about 0.15 s, which supports the statement at the end of section 4 that the proposed method is acceptable for practical applications.

We apply the proposed method to 10 more control loops in the same database, by following the same path as the control loop *cdata.chemicals.loop23*. These loops are labeled as *cdata.chemicals.loop#* with the loop no. as {2,6,7,8,9,10,11,19,20,32}. The measurements $\{u(t), y(t)\}$ and simulated outputs $\hat{y}_s(t)$ from the estimated Hammerstein systems for the 10 loops are plotted in Figure 17, together with the identified input nonlinearities and the step responses of linear subsystems. The fitness values between $y(t)$ and $\hat{y}_s(t)$ are presented in Table 1. The simulated outputs fit very well with the measured ones for these control loops. See also the results from various stiction detection techniques described in Chapter 13 of the book.[4]

Example 4. An experiment is carried out at a laboratory of Peking University, with the experimental configuration schematically depicted in Figure 18. In the experiment, the linear subsystem is a water tank system, whose cross-sectional area is about 320 cm^2. The opening position of the outlet valve is fixed. The water level of the tank system is controlled by adjusting the inlet flow via an electric control valve driven by a PI controller, $C(s) = 3(1 + (1/200s))$. The control valve becomes sticky after tightening the valve stem packing screw. The discrete-time counterpart of the PI controller $C(s)$ is implemented with the sampling period 0.5 s at a DCS platform of Siemens PCS7. Thus, a feedback control loop is formulated,

where $y(t)$, $u(t)$, and $r(t)$ stand for the water level of the tank system, the controller output, and the set point, respectively.

The collected data of process output $y(t)$, controller output $u(t)$, and set point $r(t)$ are presented in Figure 19, and divided into two data sets, the estimation data set $\{\mu(t), y(t)\}_{t=1}^{12500}$ and the validation data set $\{\mu(t), y(t)\}_{t=1}^{24800}$. On the basis of the estimation data set $\{\mu(t), y(t)\}_{t=1}^{12500}$, the proposed regularized iterative method in section 4 is applied to identify Hammerstein system, composed by the control valve followed by the water tank system. The optimal structure parameters are $\hat{n}_a = 5$, $\hat{n}_b = 2$, $\hat{n}_k = 2$, and $\hat{L} = 20$. The estimated input nonlinearity $f(\cdot)$ and the bode plot of estimated linear subsystem are shown in Figure 20. The output fitness for the estimation data set is equal to 93.5328%. To validate the identified Hammerstein model, the simulated output for the validation data set $\{\mu(t), y(t)\}_{t=12501}^{24800}$ is obtained as shown in Figure 21 with the fitness 90.4479%. Clearly, the identified Hammerstein model can well capture the main dynamic variations of $y(t)$ for both estimation and validation data sets.

For comparison, He's and Kano's stiction models are used to describe the control valve. The estimated input nonlinearities and the bode plots of estimated linear subsystem are also shown in Figure 20. The optimal structure parameters for Hammerstein system with He's stiction model are $\hat{n}_a = 3$, $\hat{n}_b = 3$, and $\hat{n}_k = 5$. The simulated outputs from Hammerstein system with He's stiction model describing the input nonlinearity, denoted by $\hat{y}_H(t)$, for the estimation and validation data sets are with fitness values 87.1078% and 82.2017%, respectively. The simulated output $\hat{y}_H(t)$ has larger discrepancies with the measured output $y(t)$ than the simulated output $\hat{y}_s(t)$ from Hammerstein system using Preisach model. Similarly, the optimal structure parameters for Hammerstein system with Kano's stiction model are $\hat{n}_a = 2$, $\hat{n}_b = 2$, and $\hat{n}_k = 5$. The simulated output from Hammerstein system using Kano's stiction model, denoted by $\hat{y}_K(t)$, for the estimation and validation data sets are with fitness values 90.8851% and 76.8164%, respectively. Note that the estimated models of linear subsystem in Figure 20 have similar dynamics in low-frequency region, so that the discrepancies among $\hat{y}_s(t)$, $\hat{y}_H(t)$, and $\hat{y}_K(t)$ are mainly caused by different models used to describe the sticky control valve. The estimated input nonlinearity using Preisach model in Figure 20 reveals that the control valve has asymmetric nonlinearity. This observation is consistent with a fact that the local oscillation amplitudes for $y(t)$ are much larger for $r(t) = 70$ than $r(t) = 30$. The comparison of simulated outputs in Figure 21 clearly shows that Preisach model is more flexible for the asymmetric nonlinearity than the data-driven stiction models.

7. CONCLUSIONS

In this Article, we introduced Preisach model as the input nonlinearity of Hammerstein system to describe sticky control valves. The discretized Preisach model is flexible; in particular, it is suitable to describe the complex characters of sticky control valves under oscillatory or more general input signals. A regularized iterative method was proposed to estimate the model parameters. The oscillatory input with only two extreme values was proved to be PE in Proposition 3 for discretized Preisach model identification. Simulated, experimental, and industrial examples support the obtained results.

One future work is to quantify the stiction severity based on the Preisach model. It is a fact that the stiction severity depends only on the valve characteristics and not on the controller
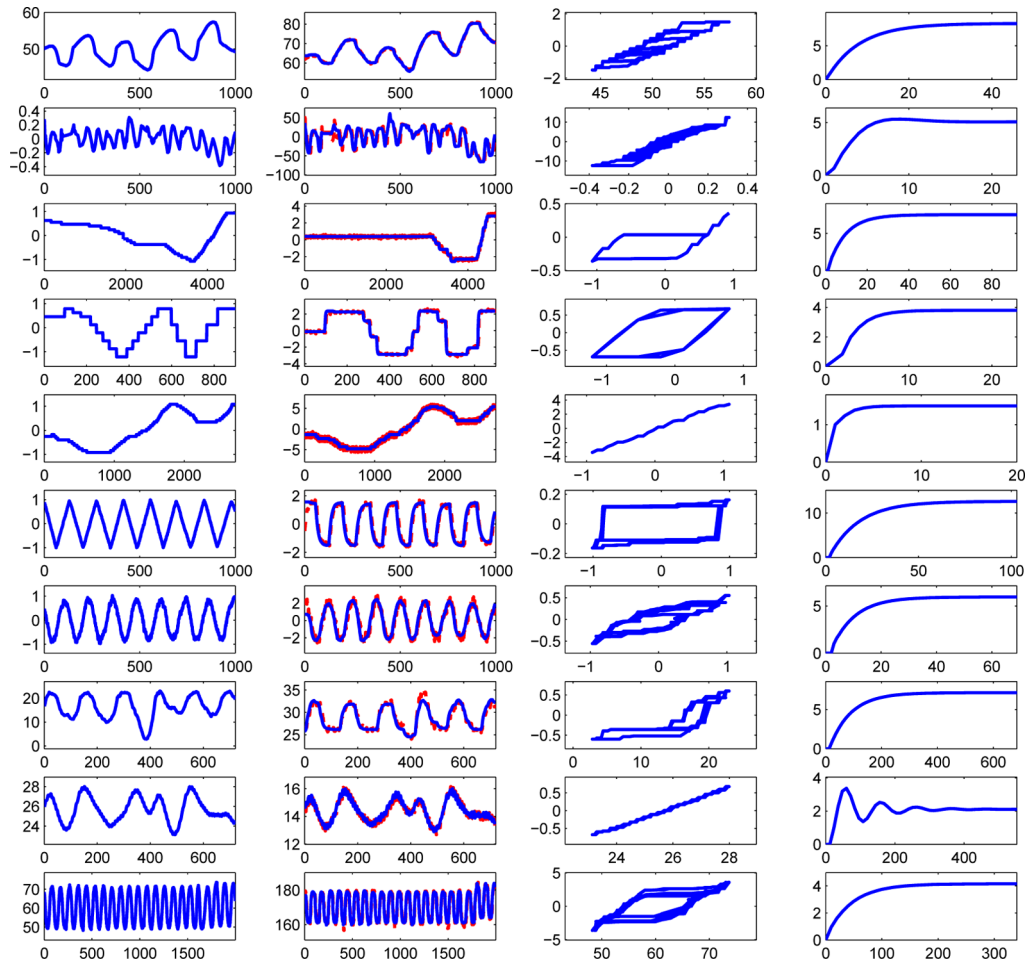
Figure 17. Time series of the input $u(t)$ (left), the measured output $y(t)$ (red - - -, middle-left) and simulated output from Hammerstein system $\hat{y}(t)$ (blue −, middle-left), the estimated input nonlinearity (middle-right), and the step response of linear subsystem (right) of loops {2,6,7,8,9,10,11,19,20,32} (from top to bottom) for Example 3.

Table 1. Fitness Values of 10 Industrial Control Loops for Example 3

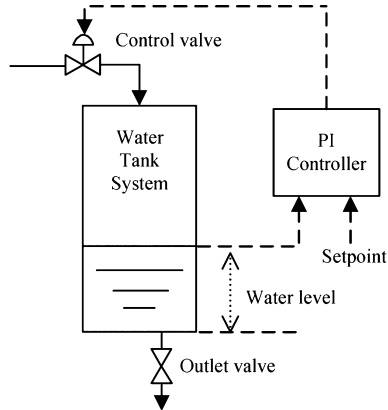| tag no.	2	6	7	8	9
fitness (%)	94.0037	74.1283	90.2817	92.9055	87.8525
tag no.	10	11	19	20	32
fitness (%)	84.5251	77.2991	72.9913	77.6292	87.8700

Figure 18. Diagram of the feedback control loop for a water tank system in Example 4.
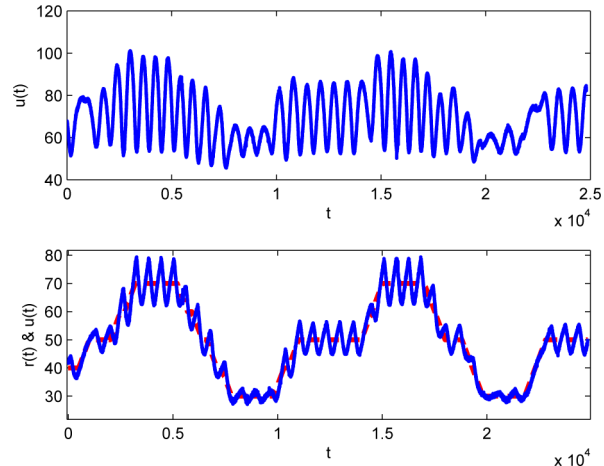

Figure 19. Input $u(t)$ (top), output $y(t)$ (bottom, blue −), and set point $r(t)$ (bottom, red - - -) of the feedback control loop for Example 4.

parameters. However, tuning the controller parameters can change the effects of stiction; for example, the amplitudes and frequencies of oscillation caused by control valve stiction can be altered by adjusting controller parameters.[45] Thus, an idea for stiction quantification is to introduce an index to measure the
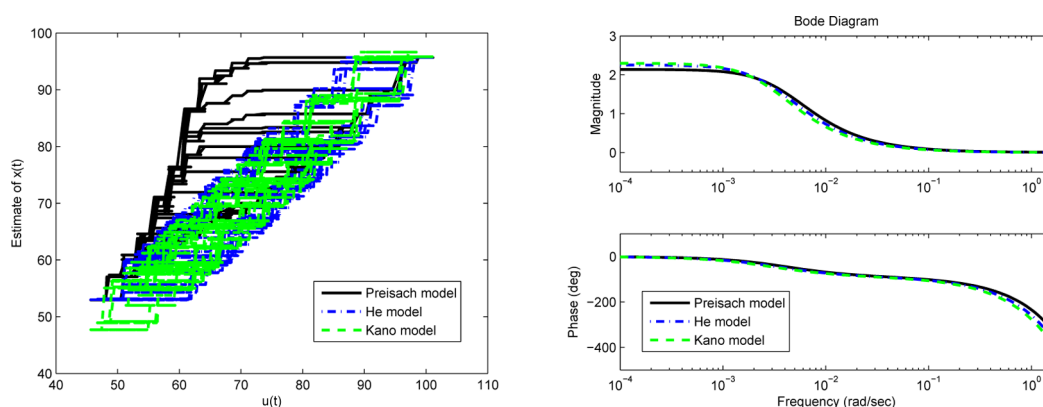
K

Figure 20. Estimated input nonlinearities (left) and the bode plots of the estimated linear subsystem (right) of Hammerstein systems using Preisach model (−), He's stiction model (blue - · - · -), and Kano's stiction model (green - - -) as input nonlinearities for Example 4.
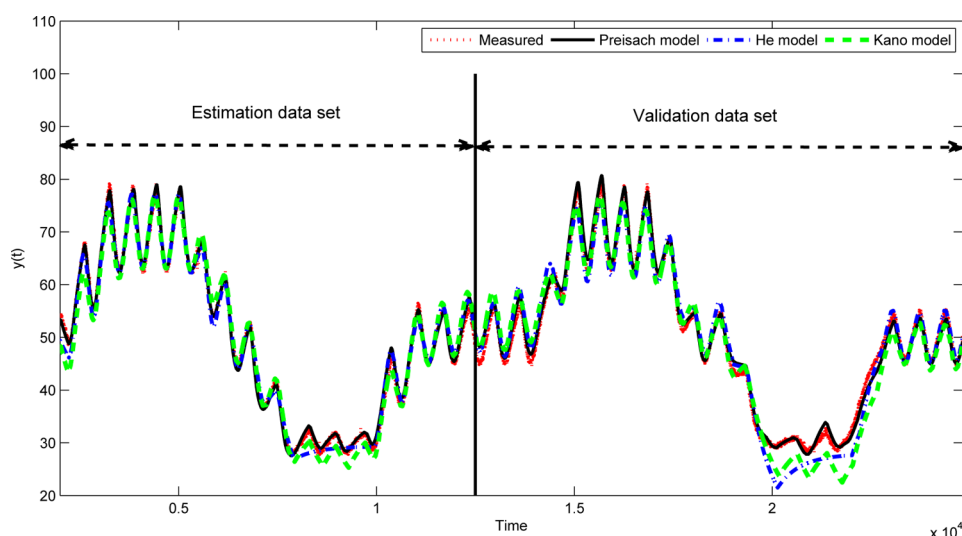

Figure 21. Comparison of the measured output $y(t)$ (red · · ·), simulated output $\hat{y}_s(t)$ (−) of Hammerstein system using Preisach model, $\hat{y}_H(t)$ (blue - · - · -) of Hammerstein system using He's stiction model, and $\hat{y}_K(t)$ (green - - -) of Hammerstein system using Kano's stiction model for the estimation and validation data sets in Example 4.

effects of control valve stiction described by the Preisach model on control loop performance.

■ AUTHOR INFORMATION

Corresponding Author

*Tel.: +86 (10) 6275-3856. Fax: +86 (10) 6275-7426. E-mail: jiandong@pku.edu.cn.

Notes

The authors declare no competing financial interest.

■ REFERENCES

(1) Bialkowski, W. L. Dreams versus reality: a view from both sides of the gap. *Pulp Pap. Can.* **1993**, *94*, 19−27.

(2) Desborough, L.; Nordh, P.; Miller, R. Control system reliability: process out of control. *Ind. Comput.* **2001**, *8*, 52−55.

(3) Paulonis, M. A.; Cox, J. A practical approach for large-scale controller performance assessment, diagnosis, and improvement. *J. Process Control* **2003**, *13*, 155−168.

(4) Jelali, M., Huang, B., Eds. *Detection and Diagnosis of Stiction in Control Loops: State of the Art and Advanced Methods*; Springer-Verlag: London, 2010.

(5) Haber, R.; Keviczky, L. *Nonlinear System Identification: Input-Output Modeling Approach*; Kluwer Academic Publishers: Dordrecht, 1999.

(6) Giri, F., Bai, E. W., Eds. *Block-Oriented Nonlinear System Identification*; Springer-Verlag: Berlin, 2010.

(7) Srinivasan, R.; Rengaswamy, R.; Narasimhan, S.; Miller, R. Control loop performance assessment. 2. Hammerstein model approach for stiction diagnosis. *Ind. Eng. Chem. Res.* **2005**, *44*, 6719−6728.

(8) Jelali, M. Estimation of valve stiction in control loops using separable least-squares and global search algorithms. *J. Process Control* **2008**, *18*, 632−642.

(9) Choudhury, M. A. A. S.; Jain, M.; Shah, S. L. Stiction−definition, modelling, detection and quantification. *J. Process Control* **2008**, *18*, 232−243.

(10) Karra, S.; Karim, M. N. Comprehensive methodology for detection and diagnosis of oscillatory control loops. *Control Eng. Practice* **2009**, *17*, 939−956.

(11) Ivan, L. Z. X.; Lakshminarayanan, S. A new unified approach to valve stiction quantification and compensation. *Ind. Eng. Chem. Res.* **2009**, *48*, 3474−3483.

(12) Qi, F.; Huang, B. Estimation of distribution function for control valve stiction estimation. *J. Process Control* **2011**, *21*, 1208−1216.

(13) Romano, R. A.; Garcia, C. Valve friction and nonlinear process model closed-loop identification. *J. Process Control* **2011**, *21*, 667−677.

(14) Farenzena, M.; Trierweiler, J. O. Valve stiction estimation using global optimization. *Control Eng. Practice* **2012**, *20*, 379−385.

(15) Capaci, R. B.; Scali, C. Stiction quantification: A robust methodology for valve monitoring and maintenance scheduling. *Ind. Eng. Chem. Res.* **2014**, *53*, 7507−7516.

(16) Nallasivam, U.; Babji, S.; Rengaswamy, R. Stiction identification in nonlinear process control loops. *Comput. Chem. Eng.* **2010**, *34*, 1890−1898.

(17) Wang, J.; Zhang, Q. Detection of asymmetric control valve stiction from oscillatory data using an extended Hammerstein system identification method. *J. Process Control* **2014**, *24*, 1−12.

(18) Cheng, Y. C.; Yu, C. C. Relay feedback identification for actuators with hysteresis. *Ind. Eng. Chem. Res.* **2000**, *39*, 4239−4249.

(19) Bai, E. W. Identification of linear systems with hard input nonlinearities of known structure. *Automatica* **2002**, *38*, 853−860.

(20) Cerone, V.; Regruto, D. Bounding the parameters of linear systems with input backlash. *IEEE Trans. Autom. Control* **2007**, *52*, 531−536.

(21) Giri, F.; Rochdi, Y.; Chaoui, F. Z.; Brouri, A. Identification of Hammerstein systems in presence of hysteresis-backlash and hysteresis-relay nonlinearities. *Automatica* **2008**, *44*, 767−775.

(22) Vörös, J. Modeling and identification of systems with backlash. *Automatica* **2010**, *46*, 369−374.

(23) Rochdi, Y.; Giri, F.; Gning, J. B.; Chaoui, F. Z. Identification of block-oriented systems in the presence of nonparametric input nonlinearities of switch and backlash types. *Automatica* **2010**, *46*, 864−877.

(24) Vörös, J. Recursive identification of nonlinear cascade systems with time-varying general input backlash. *J. Dyn. Syst., Meas., Control* **2013**, *135*, 014504−1.

(25) Giri, F.; Rochdi, Y.; Brouri, A.; Chaoui, F. Z. Parameter identification of Hammerstein systems containing backlash operators with arbitrary-shape parametric borders. *Automatica* **2011**, *47*, 1827−1833.

(26) Visintin, A. *Differential Models of Hysteresis*; Springer: New York, 1994.

(27) Brokate, M.; Sprekels, J. *Hysteresis and Phase Transitions*; Springer: New York, 1996.

(28) Mayergoyz, I. D. *Mathematical Models of Hysteresis and Their Applications*, 2nd ed.; Academic Press: New York, 2003.

(29) Ljung, L. Some classical and some new ideas for identification of linear systems. *J. Control, Autom. Electrical Syst.* **2013**, *24*, 3−10.

(30) Stenman, A.; Gustafsson, F.; Forsman, K. A segmentation-based method for detection of stiction in control valves. *Int. J. Adaptive Control Signal Process.* **2003**, *17*, 625−634.

(31) Choudhury, M. A. A.; Thornhill, N. F.; Shah, S. L. A data-driven model for valve stiction, 2004.

(32) Kano, M.; Maruta, H.; Kugemoto, H.; Shimizu, K. Practical model and detection algorithm for valve stiction, 2004.

(33) He, Q. P.; Wang, J.; Pottmann, M.; Qin, S. J. A curve fitting method for detecting valve stiction in oscillating control loops. *Ind. Eng. Chem. Res.* **2007**, *46*, 4549−4560.

(34) Fang, L.; Wang, J.; Zhang, Q. Identification of extended Hammerstein systems for modeling sticky control valves under general types of input signals. *32nd Chinese Control Conf.* **2013**, 1698−1703.

(35) Mayergoyz, I. D. Mathematical models of hysteresis. *Phys. Rev. Lett.* **1986**, *56*, 1518−1521.

(36) Banks, H. T.; Kurdila, A. J.; Webb, G. Identification of hysteretic control influence operators representing smart actuator part I: formulation. *Math. Probl. Eng.* **1997**, *3*, 287−328.

(37) Shirley, M. E.; Venkataraman, R. On the identification of Preisach measures. *Smart Struct. Mater.* **2003**, *5049*, 326−336.

(38) Iyer, R. V.; Shirley, M. E. Hysteresis parameter identification with limited experimental data. *IEEE Trans. Magn.* **2004**, *40*, 3227−3239.

(39) Tibshirani, R. Regression shrinkage and selection via the lasso. *J. R. Stat. Soc., Ser. B* **1996**, *58*, 267−288.

(40) Schwarz, G. Estimating the dimension of a model. *Ann. Stat.* **1978**, *6*, 461−464.

(41) Bai, E. W.; Li, K. Convergence of the iterative algorithm for a general Hammerstein system identification. *Automatica* **2010**, *46*, 1891−1896.

(42) Ljung, L. *System Identification: Theory for the User*, 2nd ed.; Prentice Hall: Englewood Cliffs, NJ, 1999.

(43) Tan, X.; Baras, J. S. Adaptive identification and control of hysteresis in smart materials. *IEEE Trans. Autom. Control* **2005**, *50*, 827−839.

(44) Wang, J. Closed-loop compensation method for oscillations caused by control valve stiction. *Ind. Eng. Chem. Res.* **2013**, *52*, 13006−13019.

(45) Mohammad, M.; Huang, B. Compensation of control valve stiction through controller tuning. *J. Process Control* **2012**, *22*, 1800−1819.